Metallic nanoparticles as alternative energy carriers and their combustion feasibility under ICE-like conditions

G. Karagiannakis[1], C. Mandilas[1], A.G. Konstandopoulos[1,2], C. Beatrice[3], M. Lazzaro[3], J. V. Pastor[4] and S. Molina[4]*

[1] APTL/CERTH/CPERI, P.O. Box 361, 57001 Thermi-Thessaloniki, GREECE
[2] Department of Chem.l Eng., Aristotle University, P.O. Box 1517, 54006 Thessaloniki, GREECE
[3] Istituto Motori – CNR, Viale Marconi 81056 Naples, ITALY
[4] CMT-Motores Térmicos, Universidad Politécnica de Valencia, Valencia, SPAIN

Abstract

The present work relates to the investigation of the basic oxidation characteristics of Fe and Al nanoparticles as well as to the feasibility of their combustion under Internal Combustion Engine (ICE)-like and real engine conditions. Based on a series of proof-of-concept experiments, combustion was found to be feasible taking place in a controllable way and bearing similarities to the respective case of conventional fuels. These studies were complimented by relevant in-situ and ex-situ/post-analysis, in order to elaborate the fundamental phenomena occurring during combustion as well as the extent and 'quality' of the process. The oxidation mechanisms of the two metallic fuels appear different and –as expected– the energy release during combustion of Al is significantly higher than that released in the case of Fe.

Introduction

The possibility of utilising metals as potential energy carriers and/or fuels for Internal Combustion Engines (ICE) has first been considered a few decades ago. The idea lies on two main characteristics: some metals contain significantly higher energy content per unit volume than the conventional liquid fuels, while -under certain conditions- the only product derived from their combustion is the respective metal oxide. In principle, the latter makes metals excellent candidate fuels towards the implementation of zero-emission combustion engines. The environmental friendliness of the concept can be further strengthened under the prerequisite that the metal oxide (spent fuel) is recycled so that the metal is recovered and reused. In the case of Fe and Al, their oxidation reactions can be written as follows:

$$2\cdot Fe + 1.5\cdot O_2 \rightarrow Fe_2O_3,\ \Delta H_o = -\ 826.2\ kJ/mol \quad (1)$$

$$2\cdot Al + 1.5\cdot O_2 \rightarrow Al_2O_3,\ \Delta H_o = -\ 1675.7\ kJ/mol \quad (2)$$

The fundamental problem, when considering such metals in coarse form is the fact that their ignition is difficult. However, upon ignition the combustion process proceeds in an uncontrollable way, thus resulting to extremely high temperatures which make the whole process unsuitable for ICE-like applications. This is the main reason why, until very recently, virtually all existing studies and practical applications of metal-based fuels refer to rocket propellant related applications (Li et al, 1993; Yetter et al, 2009). The most suitable way of achieving control of a metallic fuel combustion process is by tuning the size of its primary particles. Recent advances of nanotechnology in the manufacturing of metallic nanopowders with specific tailored characteristics have opened new pathways in the exploitation of such novel energy carriers. Preliminary studies indicated that, in the nanoscale regime, Fe and Al are combustible in timescales comparable with the ones of engine cycle and the phenomenon occurs either in solid or liquid state (Beach et al, 2007; Bazyn et al, 2006). The increased reactivity and controllability of nanopowders oxidation process, within reasonable ranges of temperature and pressure conditions, is attributed to their substantially high surface area (Yetter et al, 2009).

Experimental

Metallic fuels investigated in the current work included two different Fe nanopowders (one prepared by reduction of Fe_2O_3 nanopowder with H_2 and one commercially available) and an Al one. All nanopowders were subjected to proof-of-principle studies in order to exploit their fundamental engine-like and real engine combustion characteristics. The engine-like tests refer to constant-volume high-temperature vessel (combustion bomb) experiments. The combustion process in these tests was explored by means of optical diagnostic techniques. For the real

engine tests, a single cylinder compression-ignition (CI) engine was employed. The Al and one of the Fe nanopowders (referred to as Al50 and Fe50 respectively) employed in the present study were obtained from READE Advanced Materials and their purity was 99.9+%. The 2nd Fe nanopowder (referred to as Fe85) was produced via reduction with H_2 of an in-house prepared iron oxide (Fe_2O_3) nanopowder. The reduction process was followed by passivation of the resulted Fe nanoparticles (i.e formation of a thin oxide shell) to avoid undesirable spontaneous ignition. Displayed in Table 1 are characteristic parameters of the nanopowders examined along with the analytical techniques used to determine them. Representative TEM images of Fe85 and Al50 grades are depicted in Figure 1. Fe50 grade had a similar morphology to Al50 and thus is not shown. The commercial nanopowders consisted of almost spherical-shaped primary particles while the in-house Fe nanoparticles were irregularly-shaped and agglomerated.

Table 1: Main physicochemical characteristics of utilised metallic nanopowders.

Nanopowder	Estimated Average Primary Particle Size (nm)	Average thickness of oxide layer (nm)	BET (m^2/gr)	Phases identified by XRD
Fe50	50	2-3	9.3	metallic Fe
Fe85	85	2	12.7	metallic Fe
Al50	50	2-3	32.8	metallic Al

The custom-made constant volume, high-pressure, high-temperature combustion chamber system is illustrated in Figure 2. The vessel was designed to reproduce thermodynamic conditions representative to those in the cylinder of a real ICE. It was equipped with adequate optical access for visualization of the injection/combustion process. Pressure, temperature and O_2 concentration inside the vessel were fully adjustable. During the experimental process, the vessel was filled with synthetic air up to a target density and then the air was heated up with a coil heater until the target temperature was achieved. The heater was then switched off and few seconds later the metallic fuel was injected. This allowed for homogenisation of the gas temperature inside the vessel. To reduce heat loses through the walls, a refractory mortar (Greenlite 45 L) was selected for insulation. A pneumatic, powder injection system was designed with the aid of CFD analysis. In this system, nanoparticles were dragged by a gas stream capable of performing isolated injection shots of pre-defined quantities at the desired injection pressure. A shadowgraph arrangement was used for combustion imaging; images were recorded at a rate of 4·104 fps using a Phantom V12.0 high-speed camera. The engine set up is schematically shown in Figure 3. The main characteristics of the single cylinder CI ICE employed in the present study are reported in Table 2. The engine was instrumented with sensors for the required in-cylinder pressure and intake/exhaust line pressure/temperature measurements. Intake air flow was conditioned and measured by means of a custom-made air feeding system. The simplified metallic powder feeding system, placed upstream of the intake valve runner (right picture of Figure 3), was practically a nanopowder reservoir placed between a check unidirectional poppet valve and a solenoid valve, the latter connected with a low pressure (8 bar) N_2 supply line. Each “shot” of powder, synchronized with intake valve opening, inducted inside the cylinder was of a quantity sufficient to perform at least one combustion cycle. The exhaust line was equipped with a particulate filter system for the collection of combusted particles downstream of the engine.

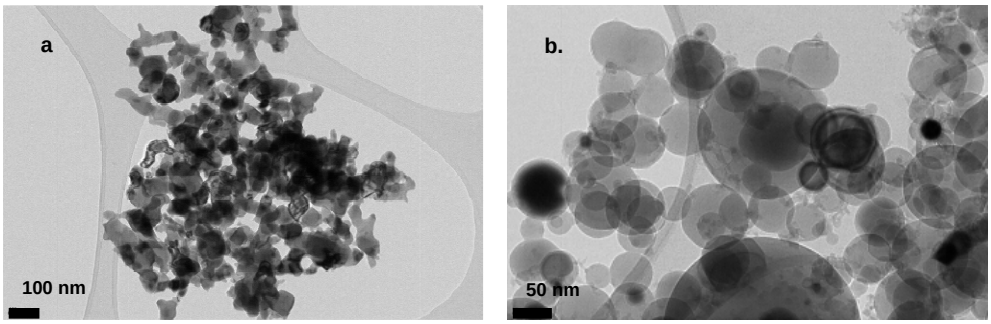

Figure 1: Indicative TEM images of nanopowders utilised: a. Fe85 and b. Al50.

Table 2: Main characteristics of the engine utilised

Property	Value/Description
Engine type	Single-cylinder Lombardini SP 15 LD 350
Displacement	350 cc
Bore/Stroke/Conrod length	82/66/110 mm

Compression ratio	20.3
Cooling system	Air

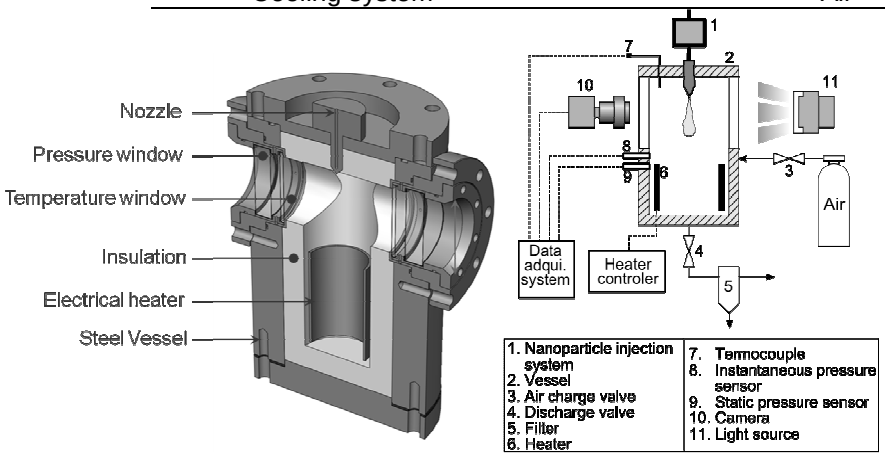

Figure 2: High-pressure, high-temperature constant volume test rig setup

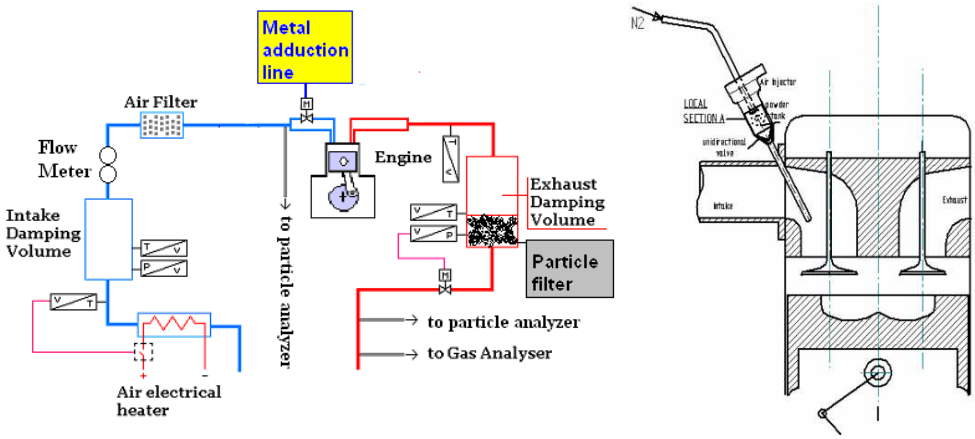

Figure 3: The engine set up utilised (left) and the nanoparticles injection system (right).

Results and Discussion

1. Combustion-bomb studies

The combustion bomb experiments provided information for the understanding of ignition and combustion of metallic nanoparticles under direct injection engine-like conditions. The direct injection system design allowed regulation of the injected quantity and therefore the percentage of particles available for combustion. One limitation is that only single injection tests could be performed. In order to replicate the P and T conditions encountered in a typical CI engine at the start of injection/early stages of ignition, bomb tests were carried out at chamber pressures between 16 and 20 bar and temperatures of up to 1073 K. The metallic nanopowders combusted in the vessel were the Fe50 and Al50 commercial grades. Injected quantities were 15 mg. Figure 4 shows a sequence of images for two single injections of Fe50 and Al50 powders respectively, at different times after the start of fuel injection. Both experiments were carried out at the same test conditions: chamber pressure of 17 bar, chamber temperature 1073 K and injection pressure of 60 bar. In the case of Fe50, it was evident that ignition occurred within very short time after the particles were injected into the combustion vessel. It is important to note that downstream of the injection point expansion caused cooling of the aerosol, which was subsequently heated up by the entrainment of hot air. Hence, in the near-to-nozzle zone only the periphery ignited. This fact was clearly observed in the relevant images, where the area near the nozzle and around the centre of the aerosol showed less luminosity. Another characteristic of the Fe50 injection-combustion tests was that the oxidation process, in terms of luminosity, evidently remained stable throughout the aerosol and during the whole injection duration. As shown in Figure 5, the pressure evolution due to Fe combustion followed a relatively smooth pattern. It was evident (Figure 4A) that penetration of the aerosol reached a

value of circa 20 mm within the first 100 μs of the injection process. At distances further than 20 mm from the nozzle only few ignited particles could be observed. These were most likely residual particles trapped at the nozzle tip during preceding tests and entrained into the chamber in the course of subsequent injections.

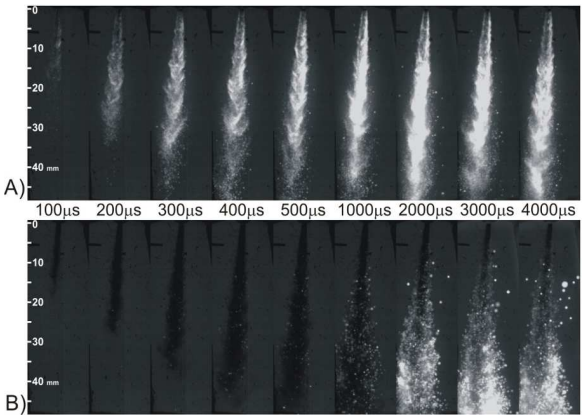

Figure 4: Frames of combustion of A) 15 mg Fe, B) 15 mg Al at 1073K

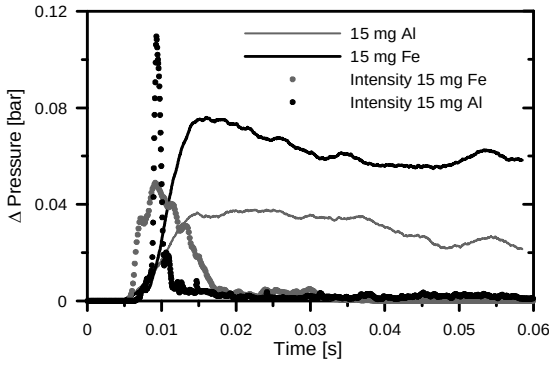

Figure 5: Pressure increase and radiation intensity for combustion tests at 1073K

With respect to Al50 combustion, a different behaviour has been determined. It was generally found that particles ignited approximately 1 ms upon injection, albeit for some cases this ignition process occurred much earlier. Al combustion proceeded with the formation of a flame of high radiation intensity, located relatively far from the nozzle. Radiation emitted by Al combustion was far more intense than that measured for Fe and the duration of the phenomenon was shorter. Ignition and combustion of Al particles within the first stage of the injection (< 2 ms) did not generate significant pressure increase. As soon as the main oxidation phase was triggered, a steep pressure increase was observed, coinciding with the radiation peak (Figure 5). Based on the fact that Al particles had higher ignition temperatures than those of Fe, the former needed more time to be heated up until the ignition point was reached, which was consistent with the image observations (Figure 4). Combustion occurred mainly on the aerosol periphery, as in the case of Fe, thus implying that mixing and air entrainment were of major importance. The latter bear similarities to the case of a typical diffusive flame observed for conventional fuel sprays. In the case of Al, it was observed that some aggregates “escaped” the bulk turbulent flow and burned remotely of the main aerosol field (i.e. as independent nuclei). Burning time of such particles was evidently longer c.f. that of the main aerosol. It could be suggested that the aforementioned aggregates were also partly due to residual powder situated at the bottom of the vessel, lifted during the combustion process due to convection. First calculations and comparisons between the pressure increase and the theoretical expected rate of heat release showed that Fe combustion was incomplete. In the case of Al, a higher percentage of unreacted metal was expected. However, further systematic studies are required.

2. Studies in Internal Combustion Engine

Included in this section are results from the CI engine tests. The engine was preliminary tested in motored conditions in order to identify the attainable compression peak pressure and temperature with respect to its geometrical characteristics. The engine results reported here refers to single powder-shot tests performed at 1500 rpm. The measurements related to the evolution of both in-cylinder pressure and temperature versus crank angle revealed peak values at the top dead center of about 40 bar and 700 K, respectively. Based on this fact, the maximum compression temperature of the selected engine was close to the burning temperature range of Al nanoparticles reported in the past (Yetter et al, 2009). As already stated, the powder injections in the intake line were preliminary adjusted in order to realise a “detectable” combustion cycle and then varied to “map” the engine response to the injected quantity of the metal. Table 4 shows the test matrix carried out in the engine experiments. Due to the fact that the simplified feeding system employed for the current tests did not provide accurate control of the actual powder mass introduced into the cylinder, the results presented contain a degree of uncertainty and should be considered as qualitative. Nevertheless, a test-to-test variability

check of the combustion cycles was carried out, indicating that the results obtained had a fair degree of repeatability. Figure 6 shows the in-cylinder pressure with the adduction of different particle quantities for both Fe85 and Al50. A fundamental observation is the fact that the introduction of the metallic nanoparticles into the cylinder generates apparent pressure and temperature increase that, in comparison to the respective values of these parameters under motored conditions, prove the feasibility of combustion under CI conditions.

Table 4: Engine test matrix.

Nanopowder	Engine speed (rpm)	Intake air temperature (°C)	Intake air mass (g per cycle)	Injected metal mass (g)	Theoretical stoichiometric air/metal fuel ratio
Fe85	1500	30	0.35	0.2, 0.3, 0.4	3.85
Al50	1500	30	0.35	0.2, 0.4	1.85

Test-to-test repeatability evaluation was conducted by performing up to 20 different tests per fuel. The results indicated a large variability in engine Indicative Mean Effective Power (IMEP). Naturally, the observed trend was largely imputable to the uncontrolled metal particle mass trapped in the cylinder. The selected sample tests in Figure 6 are proof that when appropriate in-cylinder conditions are reached (in terms of trapped particle mass and its dispersion in the cylinder), combustion occurs in a time regime comparable to that of diesel. Regarding Fe test cases (Figure 6-left), the degree of both pressure and temperature increase was proportional to the injected mass. The calculation of the heat release curves (not shown here), as rate and total energy, indicated that combustion started early in the compression stroke, evidently proceeding according to two distinct phases. Following ignition, the 1st phase of particles oxidation developed at a fast rate, suggesting that this early process was kinetically controlled. The heat release rate peaked at around 0.5 ms upon ignition, prior to descending back to values close to zero for a further ≈ 0.5 ms. A 2nd oxidation phase initiated circa 1 ms later, albeit in this case the heat release rate was notably slower. This 2nd combustion phase lasted for 4-5 ms. It should be noted that this behaviour was repeatable, however it is arguably not legitimate to speculate on the physico-chemical causes of this trend, based on the current qualitative data. The thermodynamic curves (not shown here for reason of brevity) indicate that combustion initiated at about 550K, in agreement with a previous simplified work (Beach et al, 2007).

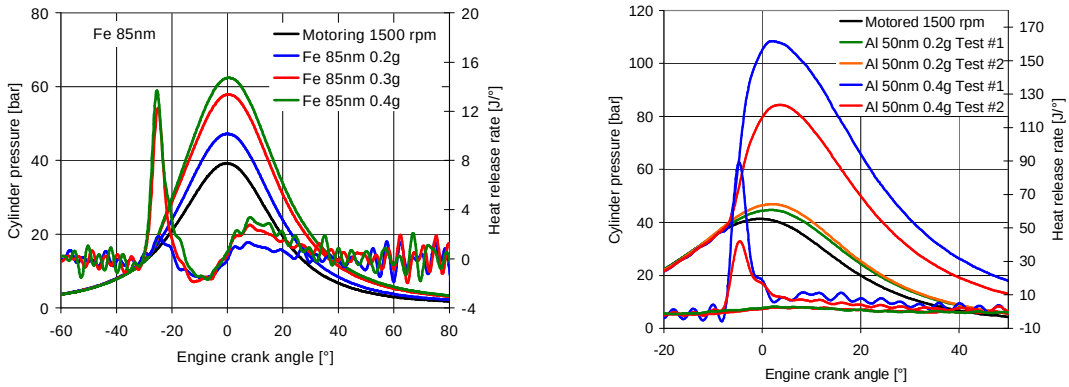

Figure 6: Cylinder pressure trace for Fe85 nm combustion (left) and for Al50 nm combustion (right). Pressure curve for motored condition is also reported. Fuel injected mass is also noted.

Qualitative conclusions drawn from Al tests were of a similar nature to those discussed earlier for Fe. Unlike Fe combustion, that of Al did not reveal two burning phases; Al50 tests showed a rapid heat release rate increase upon ignition (timescale similar to that for the 1st phase of Fe combustion) but no major heat release thereafter. Expectedly, for a given estimated amount of metal injected, the overall heat release rate for Al50 was significantly higher than Fe85. In terms of the thermodynamic gas temperature (not shown here for reasons of brevity), Al combustion started at a cylinder temperature of 600-650K. As expected, for a given amount of nanopowder, peak temperatures and pressures recorded for Al were substantially higher than the respective ones for Fe. Throughout the tests, it was found that the degree of pressure and temperature increase correlated to the estimated mass of powder injected inside the cylinder. Furthermore, the repeatability was fair. Given in Figure 7 are representative TEM images of engine-

combusted powder samples. The burned powder clusters were highly aggregated structures while, in general, oxidation was not complete as indicated by the 10-30nm thick oxide layer surrounding the (mostly) metallic Fe cores. Based on the EDS analysis, the average O/Fe ratio in both combusted Fe nanopowders samples was close to 1.0, compared to the theoretical value of 1.5 corresponding to the fully oxidised case (i.e. Fe_2O_3). On the other hand, combusted Al50 particles retained the nanostructuring of their respective unoxidised counterparts. The APPS of combusted particles, based on statistical analysis of multiple TEM images, was calculated to be approx. 80 nm, i.e. 30 nm larger than the APPS of the original sample. During the EDS analysis, no nitrogen was detected and thus formation of AlN was apparently suppressed. The combusted nanoparticles were nearly completely oxidised since the O/Al atomic ratio was measured at an average value of 1.4, while that for Al_2O_3 is known to be 1.5. It could be argued that Al particles reached the melting point of the metal and essentially burned in the liquid phase, with fast Al-O_2 mixing, substantial heat release and generation of new spherical near-completely oxidised nanoparticles upon rapid cooling.

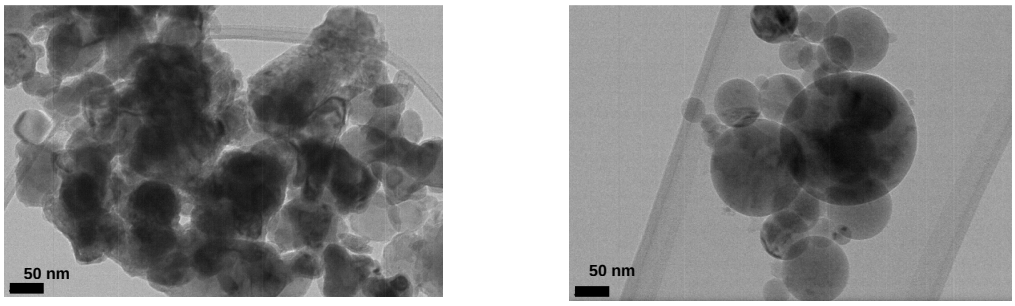

Figure 7: TEM images of samples combusted in the engine: Fe85 (left) and Al50 (right).

Conclusions

It was demonstrated that ignition and combustion of both Fe and Al nanoparticles under combustion vessel and real-engine conditions is in-principle feasible. The obtained qualitative combustion results from the single-cylinder engine, as well as those from combustion-bomb experiments, reveal that Fe nanoparticles oxidation repeatability is good and relatively ‘smooth’. Al combustion proceeds faster in comparison to that for Fe and as expected, both energy release and gas temperatures are substantially higher. Apparent differences in the combustion mechanisms of the two metals were identified. There were strong indications that Fe oxidation proceeded as a mostly solid-phase, two-phase regime evolving via thickening of oxidised/protective layer of the individual nanoparticles and formation of highly aggregated, not-fully oxidised formations. In the case of engine-combusted Al, based on relevant post-analysis, oxidation was nearly complete and the obtained spent fuel consisted of mostly-spherical nanoparticles. It should be noted that the present study refers to preliminary proof-of-principle experimental efforts. More systematic combustion studies are currently underway, with emphasis on the real-engine case. The aim is to obtain more quantitative results by controlling the powder quantity injected into the cylinder, so that detailed information on aspects such as repeatability, combustion quality as well as control of ignition and combustion rates is provided.

References

Bazyn T., H. Krier and N. Glumac (2006), Combustion of nano-aluminum at elevated pressure and temperature behind reflected shock waves, *Combustion and Flame*, 145, 703-713

Beach D.B., A. J. Rondinone, B. G. Sumpter, S. D. Labinov and R. K. Richards (2007), Solid-state combustion of metallic nanoparticles: New possibilities for an alternative energy carrier, *J. of En. Res. Techn.*, 129, 29-32.

Li S.C., F.A. Williams, K.K. Kuo and R. Pein (1993), Combustion of Boron Based Solid Propellants and Fuels, CRC Press, Boca Raton, 248-271.

Yetter R. A., G. A. Risha and S. F. Son (2009), Metal particle combustion and nanotechnology, *Proc. of the Combustion Institute*, 32, 1819-1818